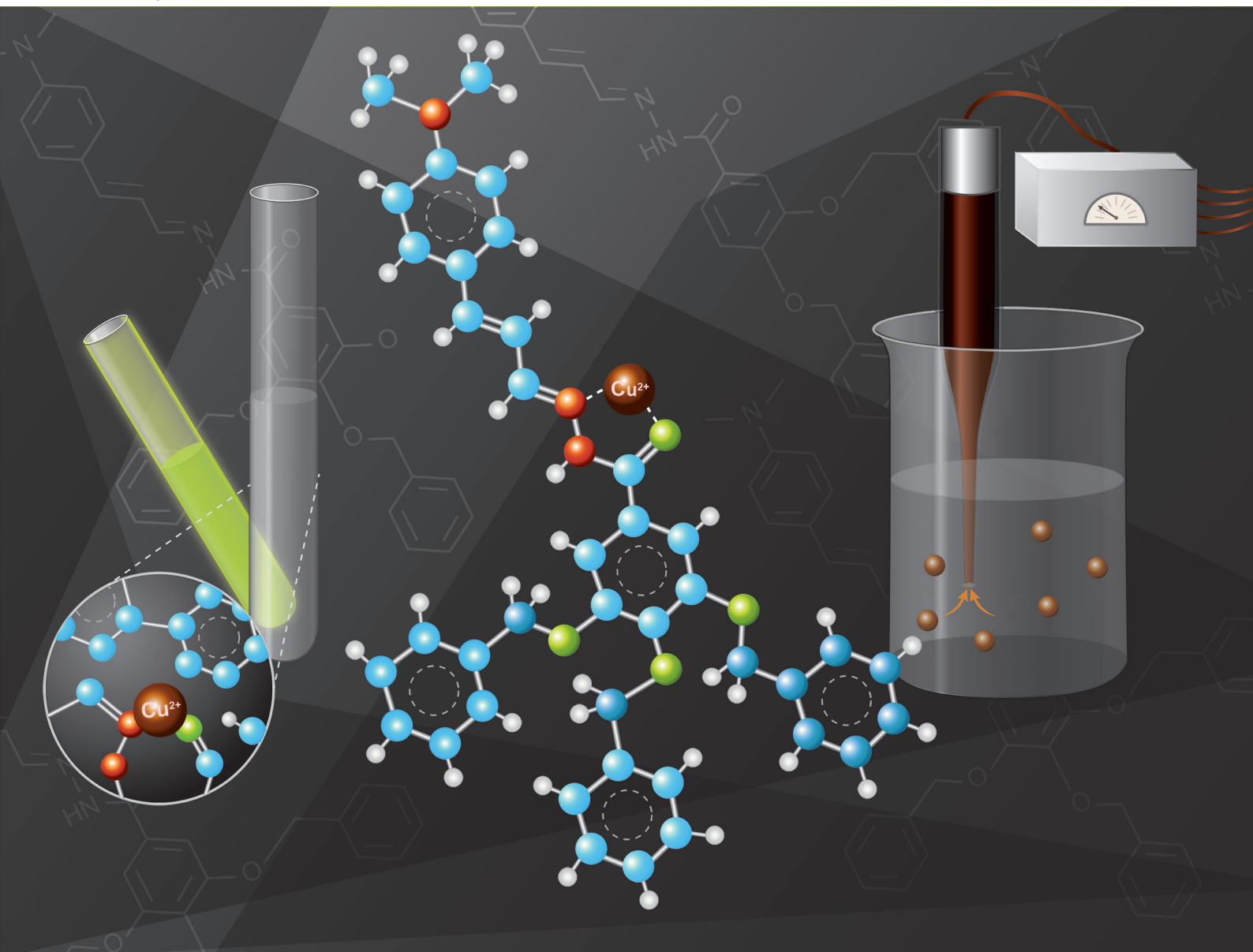


# Analyst

rsc.li/analyst



ISSN 0003-2654

**PAPER**

Dipankar Koley *et al.*

Multifunctional dendritic molecular probe for selective detection of  $\text{Cu}^{2+}$  ions using potentiometric and fluorometric techniques

## PAPER

[View Article Online](#)  
[View Journal](#) | [View Issue](#)Cite this: *Analyst*, 2021, **146**, 7109

# Multifunctional dendritic molecular probe for selective detection of Cu<sup>2+</sup> ions using potentiometric and fluorometric techniques†

Partha Sarathi Sheet,  Suji Park,  Pavel Sengupta  and Dipankar Koley \*

We have designed and synthesized a multifunctional dendritic molecular probe that selectively detects Cu<sup>2+</sup> ions *via* potentiometric and fluorometric techniques with low detection limits (3.5 μM in potentiometry, 15 nM in fluorometry). The selective and reversible binding of the molecule with the Cu<sup>2+</sup> ion was used to make a solid-state microsensor (diameter of 25 μm) by incorporating the molecular probe into the carbon-based membrane as an ionophore for Cu(II). The Cu(II) microelectrode has a broad linear range of 10 μM to 1 mM with a near Nernstian slope of 30 mV/log [a<sub>Cu<sup>2+</sup></sub>] and detection limit of 3.5 μM. The Cu(II) microsensor has a fast response time (1.5 s), and it has a broad working pH range from 3.5 to 6.0. The incorporation of the hydrophobic dendritic moiety makes the ionophore less prone to leaching in an aqueous matrix for potentiometric measurement. The cinnamaldehyde component of the molecule helps detection of Cu<sup>2+</sup> ions fluorometrically, as indicated by a change in fluorescence upon selective and reversible binding of the molecular probe to the Cu<sup>2+</sup> ions. The strategic design of the molecular probe allows us to detect Cu<sup>2+</sup> ions in drinking water by using this novel dendritic fluoroionophore and solid-state Cu<sup>2+</sup> – ion-selective microelectrode.

Received 6th August 2021,  
Accepted 22nd September 2021  
DOI: 10.1039/d1an01417j  
[rsc.li/analyst](http://rsc.li/analyst)

## 1. Introduction

Copper is a highly abundant element on Earth and has widespread use in various industries, such as electroplating, agriculture, wood preservation, and manufacturing, due to its corrosion resistance and good thermal and electrical conductivity.<sup>1,2</sup> Copper plays an essential role in many biological processes, serving as a cofactor for many enzymes and being involved in metabolism regulation and protein activation.<sup>3–5</sup> The total copper content in our body ranks third among the transition metal elements.<sup>6</sup> The concentration of Cu<sup>2+</sup> in blood serum and the synaptic cleft is 10–25 μM and 30 μM, respectively.<sup>7</sup> Nonetheless, excessive copper intake may cause Alzheimer's, Parkinson's, Wilson's, and Menkes disease.<sup>8,9</sup> According to the US Environmental Protection Agency, the allowed concentration limit of Cu<sup>2+</sup> in drinking

water is 1.3 mg L<sup>−1</sup> (20 μM).<sup>10</sup> Therefore, the detection of trace quantities of copper in various environmental and biological samples is in high demand.

Numerous analytical techniques are available to detect trace quantities of Cu<sup>2+</sup>, including atomic absorption spectrometry, inductively coupled plasma mass spectrometry, flame photometry, gravimetric detection, chromatography, fluorometry, and electrochemistry.<sup>11–20</sup> Current limitations of these analytical techniques, however, are that they require sample pretreatment; involve complicated, bulky, expensive instruments and sophisticated procedures; are time-consuming for the routine analysis of multiple environmental samples; and necessitate highly trained personnel. Also, onsite monitoring of analytes is difficult with these techniques.<sup>21,22</sup>

With a potentiometric ion-selective electrode (ISE), in contrast, analysis is simple, low cost, and portable due to its small size, which allows the ISE to be used onsite.<sup>23</sup> The most crucial component of an ISE is the ionophore embedded in its polymeric membrane, usually made up of polyvinyl chloride [PVC].<sup>24–26</sup> The ionophore has the unique capability of binding reversibly and selectively with the analyte ions.<sup>27–29</sup> In addition to the potentiometric measurements by the ionophore-based ISE, fluorometric detection of Cu(II) by using a fluorescence probe has been proven to be a versatile, selective, and sensitive method.<sup>30,31</sup>

Ying Fu *et al.* designed a 1,8-naphthalimide-based molecule, which has 320 nM of the detection limit for Cu<sup>2+</sup> detec-

Department of Chemistry, Oregon State University, Corvallis, OR 97331, USA.

E-mail: [Dipankar.Koley@oregonstate.edu](mailto:Dipankar.Koley@oregonstate.edu)

† Electronic supplementary information (ESI) available: <sup>1</sup>H, and <sup>13</sup>C NMR spectra of cinnamaldehyde modified Dendron, potentiometric response of Cu<sup>2+</sup> microsensor, cyclic voltammogram with Cu<sup>2+</sup> micro-ISE, response time of Cu(II) ion-selective electrode, comparison table for sensing performance with the commercial copper(II) ionophore I, reversibility of the CMD fluoroionophore using fluorescence and potentiometric techniques, Cu<sup>2+</sup> calibration plot for the inductively coupled plasma – optical emission spectrometry (ICP-OES). See DOI: 10.1039/d1an01417j

tion.<sup>32</sup> Minhuan Lan *et al.* also introduced the  $\text{Cu}^{2+}$  sensing performance of carbon nanoparticles with 440 nM of detection limit, and it was optimized depending on the amounts of functional groups on the surface of the nanoparticles.<sup>33</sup> More investigators have developed the fluorescence probes by synthesizing or modifying the sensing molecules.<sup>34–36</sup> However, the molecular capability of the fluorophores in the detection of single analytes using different methods often remains unexplored. We envisioned that we could quantify Cu(II) ion concentration by using a single multifunctional molecule for both potentiometry and fluorometry, instead of two separate molecules for each method. Furthermore, by incorporating a strong hydrophobic fluorophore, cinnamaldehyde derivative, into the dendron molecule, we could potentially develop a fluoroionophore for Cu(II).

To the best of our knowledge, existing Cu(II) ionophores have not been used as dual probes for potentiometry and fluorimetry. Moreover, problems have been described associated with selectivity against different metal ions, limiting their application in different areas. For example, a calixazacrown ether-based Cu(II) ionophore does not work below pH 7.0, and selectivity against common interfering ions such as alkali, alkaline earth, and most of the transition metal ions was not demonstrated; hence, it cannot be used in a situation where the pH value varies during detection.<sup>37</sup> A lariat crown ether-based Cu(II) ionophore showed a super Nernstian slope of 42 mV per decade with a slow response time of 50 s, and no selectivity values were reported for alkali and alkaline earth metal ions.<sup>38</sup> A Schiff base-based Cu(II) ionophore had poor selectivity against alkali metal (–3 or higher), alkaline earth metal (–2 or higher), transition metal ions (–1 or higher). In addition, the sensor had a slow response time (15 s). This poor selectivity will limit the use of this ionophore when it contains a high concentration of transition metal ions.<sup>39</sup> A thiaglutaric diamide-based Cu(II) ionophore had very poor selectivity toward  $\text{H}^+$ , and selectivity for most common interfering ions, such as  $\text{Fe}^{2+}$ ,  $\text{Co}^{2+}$  was not shown. These ions are known to bind to a sulfur center of an organic molecule, which will limit the use of this ionophore in water samples containing iron.<sup>40</sup> A tetrabutyl thiuram disulfide-based Cu(II) ISE has an excellent detection limit (10 nM) but is not suitable for more than a day because of decomposition of the ionophore and low selectivity against  $\text{Zn}^{2+}$  (–1.8), thus limiting the use of this ionophore in a solution containing a variable concentration of  $\text{Zn}^{2+}$ .<sup>41</sup>

Herein we report the development of a new Cu(II) ionophore molecule that is selective against major transition metal ions in addition to alkali and alkaline earth metal ions. Our molecular design incorporates reversible binding with Cu(II) by using a dendritic moiety along with an attached cinnamaldehyde component, allowing us to make a multifunctional dendritic molecular probe for the selective and sensitive detection of Cu(II). The dendritic molecular probe can act as an ionophore for potentiometric methods, and incorporation of a cinnamaldehyde moiety in the ionophore allows it to become a fluorescent molecular probe to detect  $\text{Cu}^{2+}$  ions. The selective and reversible binding of the molecule to  $\text{Cu}^{2+}$  was used to

make a solid-state micro-ISE by incorporating the multifunctional ionophore into the carbon-based membrane to detect Cu(II) with high selectivity and fast response time.

## 2. Experimental

### 2.1. Materials

All starting materials for the synthesis of cinnamaldehyde modified dendron (CMD) were obtained from Sigma-Aldrich. Vulcan carbon was a kind gift from Cabot Corporation. PVC was purchased from Aldrich. Tetramethyl silane was purchased from CIL. Potassium tetrakis(4-chlorophenyl) borate (KTCBP), sodium tetrakis [3,4-bistrifluoromethyl] phenyl borate (NaTFPB), and dioctyl sebacate (DOS) were purchased from TCI. 1-Nitro-2-(*n*-octyloxy) benzene (NPOE) was purchased from Alfa Aesar. An anion excluder, sodium tetraphenylborate (NaTPB), was obtained from Merck, and metal chlorides ( $\text{M}^{n+} = \text{Na}^+$ ,  $\text{K}^+$ ,  $\text{Mg}^{2+}$ ,  $\text{Ca}^{2+}$ ,  $\text{Cu}^{2+}$ ,  $\text{Fe}^{2+}$ ,  $\text{Co}^{2+}$ ,  $\text{Zn}^{2+}$ , and  $\text{Pb}^{2+}$ ) from TCI was used without any further purification. Deionized water (18 M $\Omega$ ) was used to make aqueous solutions.

### 2.2. Instrumentation

Amperometric measurements were performed by using a CHI potentiostat (model # 760 E, CHI, Austin, TX, USA). A three-electrode system is comprising a working electrode, an Ag/AgCl reference electrode, and a Pt wire as the counter electrode were used. Potentiometric experiments were performed with a high-impedance unit (Lawson Labs, EMF 6) along with Ag/AgCl (1 M KCl) reference electrodes.

### 2.3. Ionophore development strategy

An ionophore should reversibly bind to the analyte with high selectivity and should be insoluble in aqueous solutions to use the ISE in water samples. Since the hydrazide derivatives are known to bind with  $\text{Cu}^{2+}$  ions, we incorporated a benzo hydrazide modified dendritic structure, along with a cinnamaldehyde modification, to develop a multifunctional molecular probe for  $\text{Cu}^{2+}$  ions that will work in both potentiometry and fluorimetry. The dendritic molecular component in the molecule makes it hydrophobic, and the attached cinnamaldehyde moiety allows it to be a fluorescent molecular probe.

### 2.4. Synthesis of CMD

3,4,5-Tris(benzyloxy) benzohydrazide (2 g, 0.0044 mol) and *N,N*-dimethyl cinnamaldehyde (1.0305 g, 0.0057 mol) were dissolved in a  $\text{CHCl}_3$  (15 mL) and MeOH (45 mL) mixture. The reagent mixtures were stirred at 65 °C for 36 h under  $\text{N}_2$  atmosphere. After 36 h, the reaction mixture was concentrated *in vacuo* and the compound purified by flash chromatography over silica gel as the stationary phase. The elution was performed with 15% MeOH in  $\text{CHCl}_3$  to give the pure product as a yellow solid (experimental yield 55%).  $^1\text{H}$  NMR (700 MHz,  $\text{DMSO}-d_6$ )  $\delta$ : 2.97 (s,  $\text{CH}_3$ , 6H), 5.03 (s,  $\text{CH}_2$ , 2H), 5.21 (s,  $\text{CH}_2$ , 4H), 6.85 (dd,  $J = 8.2$  Hz, CH, 1H), 6.92 (d,  $J = 15.8$  Hz, CH, 1H), 6.72–7.50 (m, ArH & PhH, 21H), 8.20 (d,  $J = 9.2$  Hz,

CH=N, 1H), 11.47 (s, CONH, 1H) (Fig. S1†);  $^{13}\text{C}$  NMR (175 MHz, DMSO- $d_6$ )  $\delta$ : 70.91, 74.73, 107.26, 112.46, 120.95, 124.09, 128.16, 128.37, 128.44, 128.56, 128.67, 128.94, 129.28, 137.28, 137.88, 140.33, 151.13, 151.18, 152.52, 162.45 (Fig. S2†); m. p. 179 °C.

## 2.5. UV-Vis spectroscopic analysis

UV-Vis spectra of the ionophore ( $2 \times 10^{-5}$  M) were obtained in a methanol solution. The UV-Vis absorption spectrum showed a characteristic peak of cinnamaldehyde centered at 387 nm. Job's plot was obtained to quantify the metal-to-ligand binding stoichiometry. Furthermore, the binding constant was acquired in a separate experiment by varying the stoichiometry between the metal and the ligand, and the Benesi-Hildebrand plot was obtained to calculate the binding constant from the slope of the plot.

## 2.6. Fluorescence characterization and quantifications of Cu(II)

The ionophore ( $2 \times 10^{-5}$  M) showed strong fluorescence emission centered at 520 nm when excited at 387 nm. The ionophore was dissolved in methanol to make the concentration of  $2 \times 10^{-5}$  M. Then the microliter volume of the different aqueous metal ions was added to the dissolved ionophore. We tested the fluorescence response in the presence of different metal ions in a 1 : 1 mol equivalent ratio to find the selectivity of the molecular probe toward  $\text{Cu}^{2+}$ . We also obtained a calibration plot with varying concentrations of  $\text{Cu}^{2+}$  ions by using fluorescence intensity, which demonstrates the ability of the ionophore to act as a molecular fluorescence probe.

## 2.7. FT-IR characterization

The FT-IR spectrum of the 10 mM of CMD and CMD with  $\text{Cu}^{2+}$  ions (1 : 1 mol ratio) were obtained using a FT-IR spectrometer (PerkinElmer, Model: Spectrum II). The analyte solution was drop casted on a potassium bromide crystal optic disc (purchased from Alfa Aesar).

## 2.8. Fabrication of $\text{Cu}^{2+}$ microsensor

A borosilicate glass capillary (o.d. 1.5 mm, i.d. 0.86 mm) was first pulled with a pipette puller (Sutter Instruments, Novato, CA, USA), and then polished to obtain an inner tip diameter of 25  $\mu\text{m}$  ( $\text{RG} < 2$ ) to make a  $\text{Cu}^{2+}$  ion-selective microprobe. After the careful optimization of the membrane components, we have found the best ratio of the membrane components. The ion-selective cocktail was prepared by mixing 10% ionophore, 2.8% tetraphenylborate, 3% PVC, 30% DOS, 54.2% Vulcan carbon powder, and 500  $\mu\text{L}$  tetrahydrofuran (THF). The composition was mixed thoroughly with a glass rod on a watch glass until all THF evaporated. An extra 40.00% of DOS was further added to the membrane components to maintain consistency in a sensor paste. We then backfilled the pulled capillary with the sensor paste and pushed it to the pulled end with a Cu wire. To make electrical contact between the sensor paste and the inserted Cu wire, we added 5.00% Vulcan carbon in a DOS mixture to the pipette from the back-opening side. The Cu

wire connection was secured by applying 10 min epoxy to the junction of the capillary end and the Cu wire. The sensor tip was polished with lens cleaning paper and cured overnight in 1 mM  $\text{CuCl}_2$  solution before the calibration of the  $\text{Cu(II)}$  microsensor.

## 2.9. Measurement selectivity coefficients

The selectivity coefficients against different metal ions were determined by the mixed solution (fixed interference) method. Background concentrations of  $10^{-2}$  M solution for alkaline earth and transition metal cations and  $10^{-1}$  M for alkali metal cations were used.

## 2.10. Water sample preparation

The tap water samples were collected from chemistry department building at Oregon State University. The sample was appropriately diluted and pretreated by acidification and 0.2  $\mu\text{m}$  filtration since copper exists predominantly as free ionic forms or soluble ion pairs<sup>20</sup> and the measurement was carried out three times by using potentiometry, fluorimetry, and, inductively coupled plasma – optical emission spectrometry (ICP-OES) after the calibration of each method.

# 3. Results and discussion

## 3.1. Molecular design and fluorometric characterization

Our current design for the molecular probe with the cinnamaldehyde component (Fig. 1), a fluorogenic center, along with a benzo hydrazide moiety to bind with  $\text{Cu}^{2+}$ , potentially allows us to detect  $\text{Cu(II)}$  fluorometrically. To explore this possibility, we obtained the UV-Vis spectrum of the molecule. It showed the absorption band with the absorption maximum centered at 387 nm, which is characteristic of the cinnamaldehyde component of the molecule (Fig. 2A). We obtained the ligand-to-metal binding stoichiometry from the Job's plot. The data indicate that the ligand-to-metal binding ratio is 1 : 1 (Fig. 2B). The slight deviation of the ratio obtained from the Job's plot from 0.5 is possibly due to the changes in the ionic strength of the solution as the concentration of  $\text{CuCl}_2$  was increased. We also obtained the Benesi-Hildebrand plot to determine the binding constant by considering 1 : 1 metal-to-ligand binding. The calculated binding constant was  $3.51 \times 10^5 \text{ M}^{-1}$  (Fig. 2C). To demonstrate the ability of the CMD molecule ( $2 \times 10^{-5}$  M) to detect  $\text{Cu}^{2+}$  via fluorescence spectroscopy, we characterized the molecule itself by using methanol as a solvent. The CMD was simply used as a fluoroionophore in organic solvents. The fluorescence response of CMD was not studied through classical ion-selective optodes as it was beyond the scope of this study. Methanol was used as a solvent because the dendritic molecular probe is soluble in methanol but not soluble in water. Due to the different solubility behavior of the molecule, the comparison between methanol and water was avoided. The molecule showed fluorescence emission centered at 520 nm when excited at 387 nm wavelength light (Fig. 3A). For the molecule to act as a molecular probe, it should be highly selec-



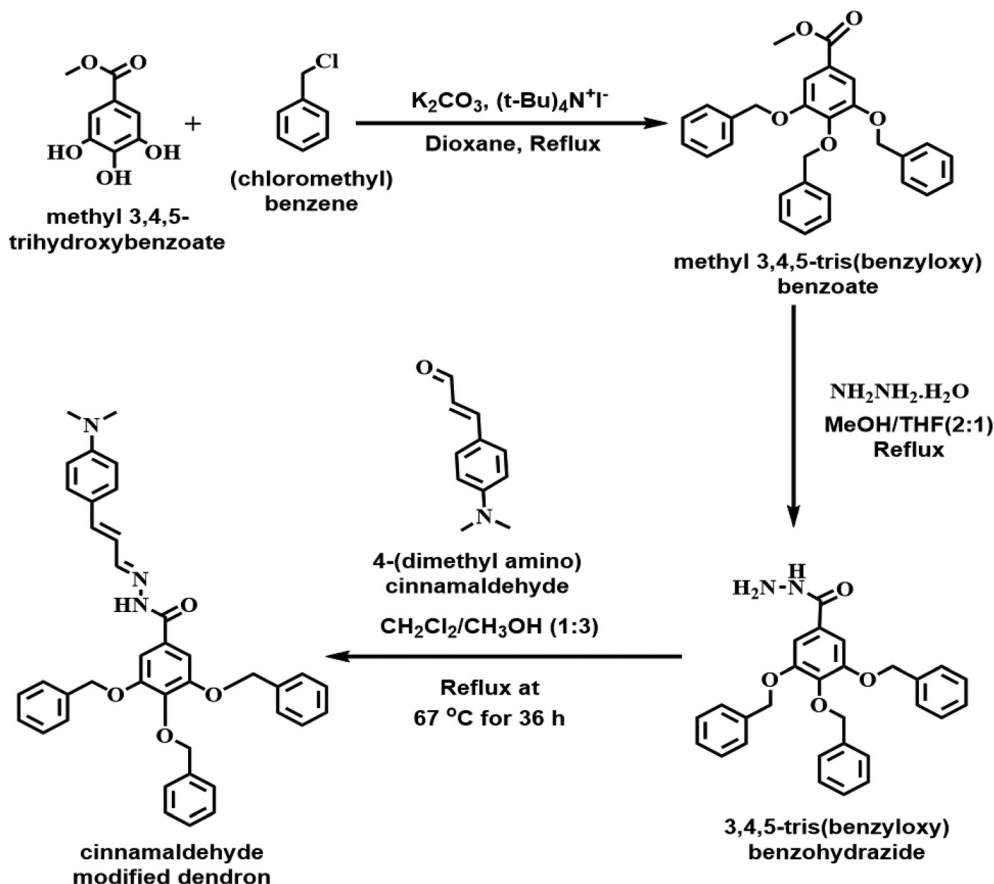


Fig. 1 Synthesis of cinnamaldehyde modified dendron ( $\text{Cu}^{2+}$  fluoroionophore).

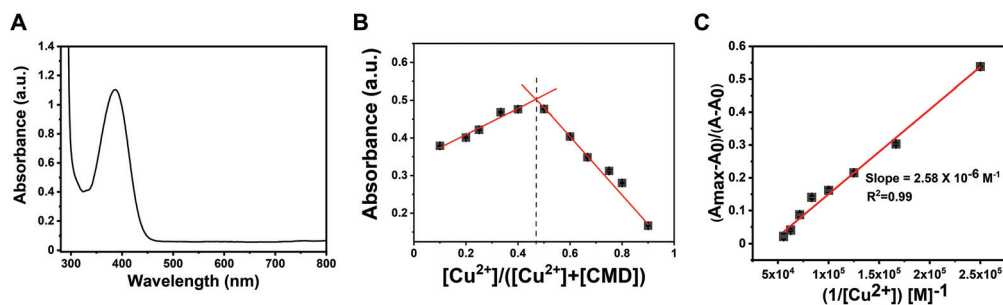
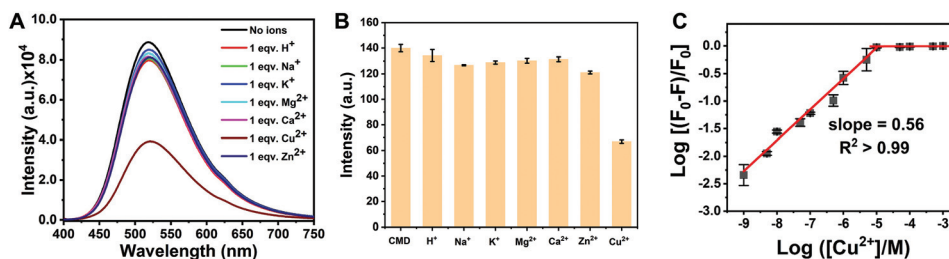


Fig. 2 UV-Vis characterization of metal–ligand binding: (A) UV-Vis spectra of the molecule ( $2 \times 10^{-5}$  M) with an absorption maximum centered at 387 nm. (B) Job's plot indicates that the ligand-to-metal binding ratio is 1 : 1 (number of experiments = 3). (C) The Benesi–Hildebrand plot provides a binding constant of the complexation ( $3.51 \times 10^5 \text{ M}^{-1}$ ) (number of experiments = 3).

tive and sensitive toward different metal ions. We tested the selectivity of CMD against different metal ions, including  $\text{H}^+$ ,  $\text{Na}^+$ ,  $\text{K}^+$ ,  $\text{Mg}^{2+}$ ,  $\text{Ca}^{2+}$ ,  $\text{Cu}^{2+}$ , and  $\text{Zn}^{2+}$  (Fig. 3B). Significant selective fluorescence quenching was observed when  $\text{Cu}^{2+}$  ions were added to the fluorophore. After the addition of various known concentrations of  $\text{Cu}^{2+}$  ions, we obtained a calibration curve, suggesting that we can use this molecule as a fluorescent molecular probe to detect and quantify  $\text{Cu}^{2+}$ . The detection limit was calculated to be 15 nM ( $\text{S/N} = 3$ ) (Fig. 3C), which is better than the other fluorescence quenching based

$\text{Cu}^{2+}$  ion selective sensors reported by Espada-Bellido *et al.* (5.6  $\mu\text{M}$ ), Weng *et al.* (1.5  $\mu\text{M}$ ), Rahimi *et al.* (3  $\mu\text{M}$ ), and Kim *et al.* (0.38  $\mu\text{M}$ ).<sup>42–45</sup>

To gain additional insights into the binding mode in the  $\text{CMD-Cu}^{2+}$  complex, we obtained the FT-IR spectrum of the free CMD (1 mM) and  $\text{CMD-Cu}^{2+}$  (1 : 1) complex in methanol (Fig. 4A and B). The characteristic  $\nu(\text{C=O})$  stretching vibrational mode appeared at  $1736 \text{ cm}^{-1}$ , and the  $\nu(\text{C=N})$  stretching vibrational mode appeared at  $1592 \text{ cm}^{-1}$  in CMD, which shows a downward shift of 10 and  $42 \text{ cm}^{-1}$ , respectively,



**Fig. 3** Fluorescence characterization of the cinnamaldehyde modified dendron (CMD)-metal complex: (A) fluorescence spectra of the molecule and in the presence of different metal ions, excitation wavelength 387 nm. (B) Interference test against metal ions (number of experiments = 3). (C) Fluorescence calibration curve for  $\text{Cu}^{2+}$  ion quantification (number of experiments = 3).

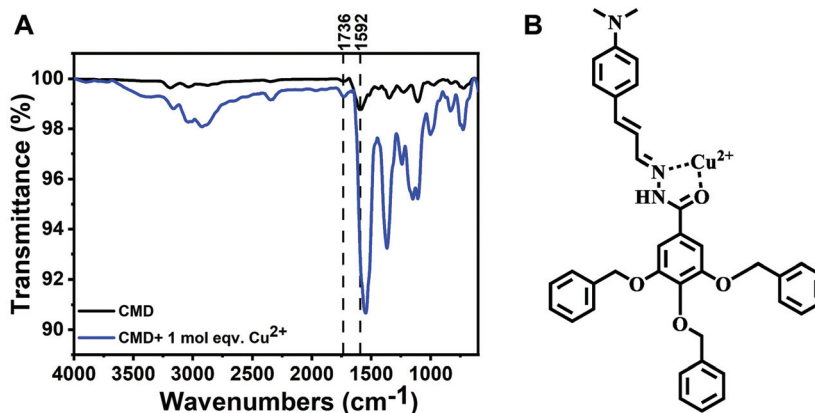


**Fig. 4** Possible mechanism of  $\text{Cu}^{2+}$  binding: (A) FT-IR spectra of the cinnamaldehyde modified dendron ionophore before and after the addition of 1 mol equiv.  $\text{Cu}^{2+}$ . (B) Possible  $\text{Cu}^{2+}$  binding site of the fluoroionophore.

in the complex form, indicating that the carbonyl oxygen and the imine nitrogen of the CMD are involved in binding.<sup>46,47</sup> Therefore, CMD acts as a bidentate ligand while complexing with the  $\text{Cu}^{2+}$  ion.

### 3.2. Potentiometric characterization of the new $\text{Cu}(\text{II})$ ionophore

We envisioned that this molecule could potentially be used as an ionophore for constructing a solid-state ISE for the detection of  $\text{Cu}(\text{II})$  *via* potentiometry. We devised a solid-state micro-ISE with the CMD as the ionophore, PVC as the binding polymer, a plasticizer, a hydrophobic anion, and Vulcan carbon, which gives a near Nernstian response of 30 mV/log  $[a_{\text{Cu}^{2+}}]$  (Fig. 5A and B). The characteristic response of the  $\text{Cu}(\text{II})$  ISE to the addition of  $\text{Cu}^{2+}$  ion is shown in Fig. S3.† The introduction of the Vulcan carbon makes the membrane conductive, potentially allowing it to be used as an amperometric probe, as shown in cyclic voltammetry (Fig. S4†). The electroactive surface area of the electrode was calculated using the voltammogram of  $\text{RuHex}$  (hexaammineruthenium(III) chloride). The calculated electroactive surface area suggests that electrode has an electroactive diameter of 23  $\mu\text{m}$  even though the geometric diameter of the electrode is 25  $\mu\text{m}$ . Unlike metal electrode, the electroactive surface area of the micro-ISE is less than the geometric surface area, which is probably due to the

presence of electro-inactive sites containing polyvinyl chloride (PVC) within the ion-selective membrane. Because of the small size of the micro-ISE, it can be used to measure  $\text{Cu}(\text{II})$  in a small volume of the sample matrix. We carefully varied the components and their amounts in the ion-selective membrane to optimize the membrane composition (Table 1). The sensors showed Nernstian slope of  $29.3 \pm 2.9$  mV/log  $[a_{\text{Cu}^{2+}}]$  and detection limits of  $3.5 \pm 1.0$   $\mu\text{M}$  (Table 1). The incorporation of a plasticizer plays a vital role in a PVC-based ISE, since it can provide ionic mobility within the membrane. We compared the performance of two different plasticizers, NPOE and DOS in the present membrane. As shown in Table 1, a better slope of the sensor is obtained by incorporating DOS. The performance of the plasticizer usually depends on the dielectric constants and DOS has a relatively lower value of it. A hydrophobic counter anion is often included into the membrane to facilitate cation extraction within the membrane, reduce ohmic resistance, and improve response behavior. We compared different lipophilic anions such as KTCBP, NaTFPB, and NaTPB for the construction of the micro-ISE and found that the slope was worst for NaTFPB. In contrast, NaTPB showed the best response because of its better ion extraction ability and the optimum lipophilic anion to ionophore mole ratio which was 0.5. TPB is a stronger ion exchanger due to the absence of electronegative halides (has negative inductive

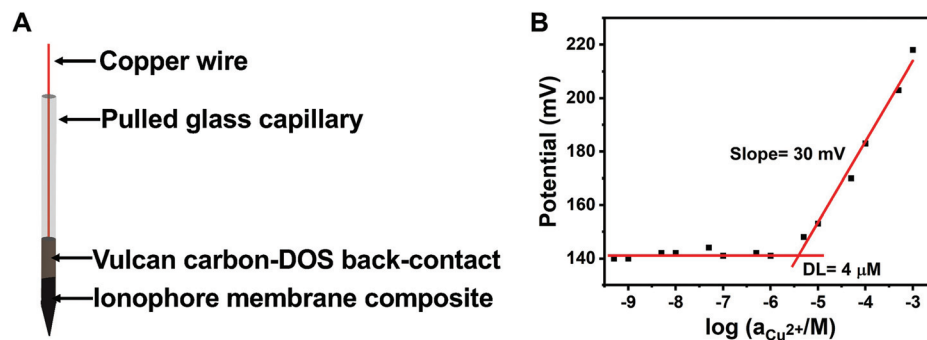


**Fig. 5** Potentiometric characterization of the  $\text{Cu}^{2+}$  ISE: (A) schematic of the carbon-packed  $\text{Cu}(\text{II})$  microsensor. (B) Potentiometric calibration of  $\text{Cu}^{2+}$  with the carbon-packed sensor. DOS: dioctyl sebacate. The sensors showed Nernstian slope of  $29.3 \pm 2.9$  mV/log  $[\text{a}_{\text{Cu}^{2+}}]$  and detection limits of  $3.5 \pm 1.0$   $\mu\text{M}$  (number of experiments = 6).

**Table 1** Composition and characterization of carbon-packed sensors, including slope, linear range, and detection limit (number of experiments = 6)

I (%)	LA (%)	Plasticizer (%)	PVC (%)	VC (%)	Molar ratio (LA : I)	Linear range (M)	Slope (mV/log $[\text{a}_{\text{Cu}^{2+}}]$ )	DL ( $\mu\text{M}$ )
6.9	KTCBP (2.0)	NPOE (30)	3	58.1	0.3	$10^{-5}$ – $10^{-3}$	$11.8 \pm 4.2$	$13.8 \pm 1.8$
6.9	KTCBP (3.3)	NPOE (30)	3	56.8	0.6	$10^{-5}$ – $10^{-3}$	$12.5 \pm 1.3$	$11.1 \pm 0.8$
6.9	KTCBP (1.4)	DOS (30)	3	56.8	0.2	$10^{-5}$ – $10^{-3}$	$14.8 \pm 2.5$	$10.0 \pm 3.3$
6.9	KTCBP (3.3)	DOS (30)	3	56.8	0.6	$10^{-5}$ – $10^{-3}$	$17.2 \pm 3.0$	$7.8 \pm 2.2$
10	KTCBP (3.5)	DOS (30)	3	53.5	0.4	$10^{-5}$ – $10^{-3}$	$16.0 \pm 1.0$	$9.6 \pm 0.9$
10	KTCBP (4.5)	DOS (30)	3	52.5	0.6	$10^{-5}$ – $10^{-3}$	$19.4 \pm 0.5$	$16.2 \pm 2.5$
10	NaTFPB (6.0)	DOS (30)	3	51.0	0.4	$10^{-5}$ – $10^{-3}$	$15.0 \pm 3.6$	$334.1 \pm 105.8$
7	NaTPB (2.0)	DOS (30)	3	58.0	0.5	$10^{-5}$ – $10^{-3}$	$7.1 \pm 2.8$	$54.2 \pm 34.7$
10	NaTPB (1.4)	DOS (30)	3	55.6	0.3	$10^{-5}$ – $10^{-3}$	$23.6 \pm 7.2$	$3.0 \pm 1.0$
10	NaTPB (2.8)	DOS (30)	3	54.2	0.5	$10^{-5}$ – $10^{-3}$	$29.3 \pm 2.9$	$3.5 \pm 1.0$

I: ionophore; LA: lipophilic anion; PVC: polyvinyl chloride; VC: Vulcan carbon; DL: detection limit; KTCBP: potassium tetrakis(4-chlorophenyl) borate; NaTFPB: sodium tetrakis [3,4-bistrifluoromethyl phenyl] borate; NaTPB: sodium tetraphenylborate; NPOE: 1-nitro-2-(*n*-octyloxy) benzene; DOS: dioctyl sebacate.

effect) which makes the electron localization on the boron atom leads to stronger ion-pair formation with the analyte.<sup>48</sup> After careful investigation of the membrane components, we optimized the composition of ISE membrane as 10% ionophore, 2.8% tetraphenylborate, 3% PVC, 30% DOS, and 54.2% Vulcan carbon, which gives a Nernstian response of  $29.3 (\pm 2.9)$  mV/log  $[\text{a}_{\text{Cu}^{2+}}]$  (linear range 10  $\mu\text{M}$  to 1 mM) with a detection limit of  $3.5 (\pm 1.0)$   $\mu\text{M}$ .

Later, the effect of pH on the sensor was measured in the presence of  $10^{-3}$  M  $\text{CuCl}_2$ . The pH of the solution was adjusted by using either 0.1 M HCl or 0.1 M NaOH. Fig. 6A shows the effect of pH on the response in potential by the  $\text{Cu}(\text{II})$  microsensor. The potential remains constant within the pH range from 3.5 to 6.0 for the microsensor. The response in potential outside this range is due to interference by  $\text{H}^+$  at the low end of the pH scale and  $\text{Cu}(\text{OH})_2$  formation at the higher end of the pH scale. Therefore, the working pH range for the present electrode is from 3.5 to 6.0. The activity was obtained by only considering the presence of  $\text{Cu}^{2+}$  and  $\text{Cl}^-$  in the system. Formation of complexes like  $\text{Cu}(\text{OH})^+$  and  $\text{CuCl}^+$  was not taken into account because working pH range for the ISE is from 3.5 to 6.0 and within this pH range, the aqueous solution of  $\text{CuCl}_2$  exists primarily as  $\text{Cu}^{2+}$  and  $\text{Cl}^-$ .<sup>49,50</sup> Furthermore, we used the

complexation behavior of the molecule as an ionophore in an ion-selective membrane-based electrode. The selectivity test was performed with different metal ions such as  $\text{H}^+$ ,  $\text{Na}^+$ ,  $\text{K}^+$ ,  $\text{Mg}^{2+}$ ,  $\text{Ca}^{2+}$ ,  $\text{Fe}^{2+}$ ,  $\text{Co}^{2+}$ ,  $\text{Zn}^{2+}$ , and  $\text{Pb}^{2+}$ . The ion-selective membrane electrode shows high selectivity toward  $\text{Cu}^{2+}$  ions and the selectivity coefficients were calculated as  $\log K_{\text{Cu}^{2+}, \text{A}} \leq -2.13, -3.80, -3.15, -3.42, -3.09, -2.55, -3.10, -3.00$ , and  $-2.21$ , respectively. The selectivity values for most of the metal ions were found to be  $\leq -3$ , which is an improvement of almost one order of magnitude over the commercially available  $\text{Cu}(\text{II})$  ionophore-I<sup>51</sup> (Fig. 6B). The sensor was also compared with the sensor containing commercially available  $\text{Cu}(\text{II})$  ionophore I in terms of detection limit, slope, response time, and pH range (Table S1†). Fig. S5† represents a response time of 1.5 s obtained from the  $\text{Cu}(\text{II})$  ISE. The reversibility of the sensors was carefully investigated using potentiometric and fluorometric techniques. The reversibility of the  $\text{Cu}(\text{II})$  sensor was demonstrated using both techniques in Fig. S6† and its description. The ionophore shows reversible behavior in both potentiometric and fluorometric modes.

### 3.3. Detection of $\text{Cu}^{2+}$ in tap water

We used the newly developed  $\text{Cu}(\text{II})$  micro-ISE to measure the amount of copper present in tap water collected from the main

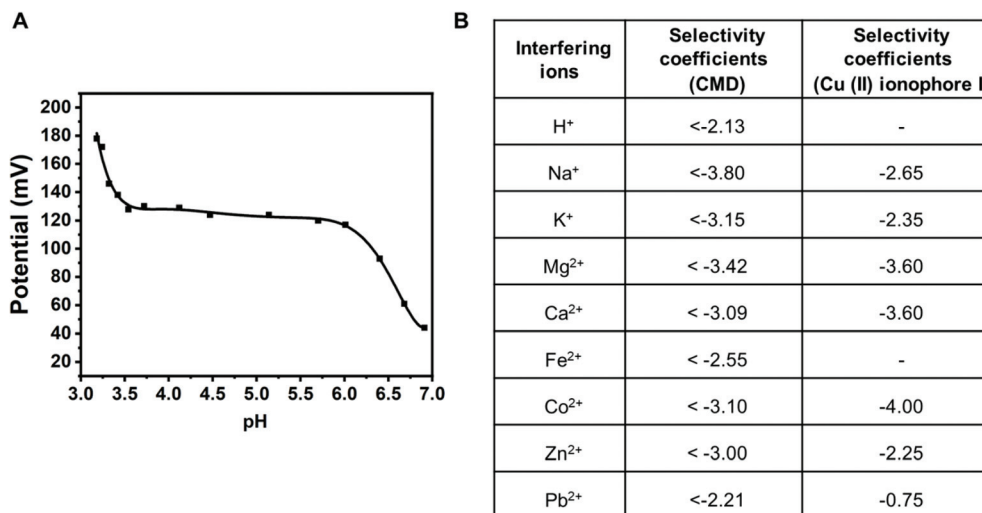


**Fig. 6** (A) Effect of pH on the carbon-packed sensor using the CMD ionophore. (B) The selectivity coefficients table of the carbon-packed sensor using the CMD ionophore is compared against the commercial ionophore (copper(II) ionophore I<sup>51</sup>). The selectivity coefficients for both the ionophores were obtained using the fixed interference method.

**Table 2** Water samples collected, and the amount of Cu<sup>2+</sup> was found in samples by using a Cu<sup>2+</sup> ion-selective electrode (ISE), fluorimetry, and inductively coupled plasma – optical emission spectrometry (ICP-OES) (number of experiments = 3)

Water sample	ISE	Fluorimetry	ICP-OES
Tap water in Gilbert Hall	38.0 ±	38.9 ±	38.0 ±
Addition at Oregon State University	1.7 μM	0.9 μM	0.9 μM

campus of Oregon State University (OSU). The CMD ionophore was also used as a fluorometric Cu(II) sensor to measure the amount of Cu<sup>2+</sup> in the same tap water sample. Further, we have compared the results of the quantitative analysis with those of inductively coupled plasma – optical emission spectrometry (ICP-OES) as a standard technique (Table 2). The calibration plot obtained with ICP-OES is shown in Fig. S7.† The amount of Cu(II) present in OSU campus (Gilbert Addition) tap water was found to be 38.0 ± 1.7 μM using ISE, 38.9 ± 0.9 μM using fluorimetry, and 38.0 ± 0.9 μM from ICP-OES. This indicates that we can reliably measure the amount of copper present in water samples by using this CMD fluoroionophore. The agreement of Cu<sup>2+</sup> concentrations obtained from three different methods also suggests that contribution from complexes is minimal by acidification of tap water samples.

## 4. Conclusions

We have successfully designed and synthesized a novel molecular probe to detect Cu(II) by using both potentiometric and fluorometric methods. With the fluorometric technique, we can detect up to 15 nM Cu<sup>2+</sup>, and it shows selectivity toward

Cu<sup>2+</sup> ions when tested against common metal ions such as H<sup>+</sup>, Na<sup>+</sup>, K<sup>+</sup>, Ca<sup>2+</sup>, Mg<sup>2+</sup>, and Zn<sup>2+</sup>. The molecular probe was used as an ionophore to develop a carbon-based solid-state micro-ISE to detect Cu(II) in the drinking water sample. The selectivity of the ionophore represents an improvement of at least one order of magnitude over the commercial ionophore and has a fast response time (1.5 s). With its improved selectivity and response time, this microsensor can be used to detect Cu(II) ions in micro-volumes, which also makes it compatible with scanning electrochemical microscopy (SECM). Current studies are underway in the laboratory to use the ionophore as a Cu(II) micro-ISE probe for SECM studies besides exploring the possibility of using this molecule as an optode by recording fluorescence response from the PVC based ion-selective membrane.

## Conflicts of interest

There are no conflicts to declare.

## Acknowledgements

We thank the National Institute of Dental and Craniofacial Research as a funding agency, NIH Grant No. R01DE027999 (D. K.). We also thank Dr. Chong Fang and Dr. Cheng Chen at Oregon State University for their help in using the fluorometer. The authors also acknowledge Dr. Chris J. Russo, Lab Manager at the Keck Collaboratory for Plasma Spectrometry, Oregon State University for aiding in ICP-OES data acquisition and interpretation. We would also like to thank Chris Bahro, Bronson Samel-Garloff, Anh Tuan Nguyen, and Dr. Subir Goswami for their useful suggestions.



## References

- 1 V. K. Gupta, R. Prasad and A. Kumar, Preparation of ethambutol-copper(II) complex and fabrication of PVC based membrane potentiometric sensor for copper, *Talanta*, 2003, **60**, 149–160, DOI: 10.1016/S0039-9140(03)00118-8.
- 2 V. K. Gupta, L. P. Singh, R. Singh, N. Upadhyay, S. P. Kaur and B. Sethi, A novel copper(II) selective sensor based on Dimethyl 4, 4' (o-phenylene) bis(3-thioallophanate) in PVC matrix, *J. Mol. Liq.*, 2012, **174**, 11–16, DOI: 10.1016/j.molliq.2012.07.016.
- 3 E. L. Que, D. W. Domaille and C. J. Chang, Metals in neurobiology: Probing their chemistry and biology with molecular imaging, *Chem. Rev.*, 2008, **108**, 1517–1549, DOI: 10.1021/cr078203u.
- 4 J. R. Prohaska and A. A. Gybina, Recent Advances in Nutritional Sciences Intracellular Copper Transport in Mammals, *J. Nutr.*, 2004, **134**, 1003–1006.
- 5 E. I. Solomon, D. E. Heppner, E. M. Johnston, J. W. Ginsbach, J. Cirera, M. Qayyum, M. T. Kieber-Emmons, C. H. Kjaergaard, R. G. Hadt and L. Tian, Copper active sites in biology, *Chem. Rev.*, 2014, **114**, 3659–3853, DOI: 10.1021/cr400327t.
- 6 E. Gaggelli, H. Kozlowski, D. Valensin and G. Valensin, Copper homeostasis and neurodegenerative disorders (Alzheimer's, prion, and Parkinson's diseases and amyotrophic lateral sclerosis), *Chem. Rev.*, 2006, **106**, 1995–2044, DOI: 10.1021/cr040410w.
- 7 A. I. Bush, Metals and neuroscience, *Curr. Opin. Chem. Biol.*, 2000, **4**, 184–191, DOI: 10.1016/S1367-5931(99)00073-3.
- 8 K. J. Barnham, C. L. Masters and A. I. Bush, Neurodegenerative diseases and oxidative stress, *Nat. Rev. Drug Discovery*, 2004, **3**, 205–214, DOI: 10.1038/nrd1330.
- 9 P. C. Bull and D. W. Cox, Wilson disease and Menkes disease: new handles on heavy-metal transport, *Trends Genet.*, 1994, **10**, 246–252, DOI: 10.1016/0168-9525(94)90172-4.
- 10 U.S. Environmental Protection Agency, *Drinking Water Contaminants*, U.S. EPA, 2009, pp. 1–14.
- 11 C. Karadaş and D. Kara, Dispersive liquid–liquid microextraction based on solidification of floating organic drop for preconcentration and determination of trace amounts of copper by flame atomic absorption spectrometry, *Food Chem.*, 2017, **220**, 242–248, DOI: 10.1016/j.foodchem.2016.09.005.
- 12 Z. Wei, S. Sandron, A. T. Townsend, P. N. Nesterenko and B. Paull, Determination of trace labile copper in environmental waters by magnetic nanoparticle solid phase extraction and high-performance chelation ion chromatography, *Talanta*, 2015, **135**, 155–162, DOI: 10.1016/j.talanta.2014.12.048.
- 13 J. Wu and E. A. Boyle, Low Blank Preconcentration Technique for the Determination of Lead, Copper, and Cadmium in Small-Volume Seawater Samples by Isotope Dilution ICPMS, *Anal. Chem.*, 1997, **69**, 2464–2470, DOI: 10.1021/ac961204u.
- 14 N. M. Galloway, Flame-photometric determination of iron, copper and cobalt in cobalt mattes and concentrates, *Analyst*, 1959, **84**, 505–508, DOI: 10.1039/AN9598400505.
- 15 H. Yu, P. Xu, D. W. Lee and X. Li, Porous-layered stack of functionalized AuNP-rGO (gold nanoparticles-reduced graphene oxide) nanosheets as a sensing material for the micro-gravimetric detection of chemical vapor, *J. Mater. Chem. A*, 2013, **1**, 4444–4450, DOI: 10.1039/c3ta01401k.
- 16 A. Ali, H. Shen and X. Yin, Simultaneous determination of trace amounts of nickel, copper and mercury by liquid chromatography coupled with flow-injection on-line derivatization and preconcentration, *Anal. Chim. Acta*, 1998, **369**, 215–223, DOI: 10.1016/S0003-2670(98)00252-9.
- 17 C. F. B. Coutinho, L. F. M. Coutinho, L. H. Mazo, S. L. Nixdorf, C. A. P. Camara and F. M. Lanças, Direct determination of glyphosate using hydrophilic interaction chromatography with coulometric detection at copper microelectrode, *Anal. Chim. Acta*, 2007, **592**, 30–35, DOI: 10.1016/j.aca.2007.04.003.
- 18 H. Q. Chen, A. N. Liang, L. Wang, Y. Liu and B. B. Qian, Ultrasensitive determination of Cu<sup>2+</sup> by synchronous fluorescence spectroscopy with functional nanoparticles, *Microchim. Acta*, 2009, **164**, 453–458, DOI: 10.1007/s00604-008-0082-6.
- 19 G. Zhao, R. Liang, F. Wang, J. Ding and W. Qin, An all-solid-state potentiometric microelectrode for detection of copper in coastal sediment pore water, *Sens. Actuators, B*, 2019, **279**, 369–373, DOI: 10.1016/j.snb.2018.09.125.
- 20 S. Park, C. S. Maier and D. Koley, Anodic Stripping Voltammetry on a Carbon-based Ion-Selective Electrode, *Electrochim. Acta*, 2021, 138855, DOI: 10.1016/j.electacta.2021.138855.
- 21 A. K. Singh, S. Mehtab and A. K. Jain, Selective electrochemical sensor for copper(II) ion based on chelating ionophores, *Anal. Chim. Acta*, 2006, **575**, 25–31, DOI: 10.1016/j.aca.2006.05.076.
- 22 S. W. Huang, Y. F. Lin, Y. X. Li, C. C. Hu and T. C. Chiu, Synthesis of fluorescent carbon dots as selective and sensitive probes for cupric ions and cell imaging, *Molecules*, 2019, **24**, 1–12, DOI: 10.3390/molecules24091785.
- 23 A. Paul, R. R. Nair, P. B. Chatterjee and D. N. Srivastava, Fabrication of a Cu(II)-Selective Electrode in the Polyvinyl Chloride Matrix Utilizing Mechanochemically Synthesized Rhodamine 6 g as an Ionophore, *ACS Omega*, 2018, **3**, 16230–16237, DOI: 10.1021/acsomega.8b02870.
- 24 E. Bakker, P. Bühlmann and E. Pretsch, Carrier-based ion-selective electrodes and bulk optodes. 1. General characteristics, *Chem. Rev.*, 1997, **97**, 3083–3132, DOI: 10.1021/cr940394a.
- 25 J. Bobacka, A. Ivaska and A. Lewenstam, Potentiometric ion sensors, *Chem. Rev.*, 2008, **108**, 329–351, DOI: 10.1021/cr068100w.
- 26 V. S. Joshi, P. S. Sheet, N. Cullin, J. Kreth and D. Koley, Real-Time Metabolic Interactions between Two Bacterial Species Using a Carbon-Based pH Microsensor as a Scanning Electrochemical Microscopy Probe, *Anal. Chem.*,

- 2017, **89**, 11044–11052, DOI: 10.1021/acs.analchem.7b03050.
- 27 R. D. Johnson and L. G. Bachas, Ionophore-based ion-selective potentiometric and optical sensors, *Anal. Bioanal. Chem.*, 2003, **376**, 328–341, DOI: 10.1007/s00216-003-1931-0.
  - 28 E. Bakker, Electrochemical sensors, *Anal. Chem.*, 2004, **76**, 3285–3298, DOI: 10.1021/ac049580z.
  - 29 J. G. Ummadi, C. J. Downs, V. S. Joshi, J. L. Ferracane and D. Koley, Carbon-Based Solid-State Calcium Ion-Selective Microelectrode and Scanning Electrochemical Microscopy: A Quantitative Study of pH-Dependent Release of Calcium Ions from Bioactive Glass, *Anal. Chem.*, 2016, **88**, 3218–3226, DOI: 10.1021/acs.analchem.5b04614.
  - 30 H. Chen, J. Zhu, X. Cao and Q. Fang, Flow injection on-line photochemical reaction coupled to spectrofluorimetry for the determination of thiamine in pharmaceuticals and serum, *Analyst*, 1998, **123**, 1017–1021, DOI: 10.1039/a708762d.
  - 31 N. Yadav and A. K. Singh, Colorimetric and Fluorometric Detection of Heavy Metal Ions in Pure Aqueous Medium with Logic Gate Application, *J. Electrochem. Soc.*, 2019, **166**, B644–B653, DOI: 10.1149/2.1341906jes.
  - 32 Y. Fu, X. X. Pang, Z. Q. Wang, Q. Chai and F. Ye, A highly sensitive and selective fluorescent probe for determination of Cu(II) and application in live cell imaging, *Spectrochim. Acta, Part A*, 2019, **208**, 198–205, DOI: 10.1016/j.saa.2018.10.005.
  - 33 M. Lan, S. Zhao, S. Wu, X. Wei, Y. Fu, J. Wu, P. Wang and W. Zhang, Optically tunable fluorescent carbon nanoparticles and their application in fluorometric sensing of copper ions, *Nano Res.*, 2019, **12**, 2576–2583, DOI: 10.1007/s12274-019-2489-2.
  - 34 J. Wang, J. Yu, X. Wang, L. Wang, B. Li, D. Shen, Q. Kang and L. Chen, Functional ZnS:Mn(II) quantum dot modified with L-cysteine and 6-mercaptopurine as a fluorometric probe for copper(II), *Microchim. Acta*, 2018, **185**, 420, DOI: 10.1007/s00604-018-2952-x.
  - 35 L. Lu, G. Yang and Y. Xia, From Pair to single: Sole fluorophore for ratiometric sensing by dual-emitting quantum dots, *Anal. Chem.*, 2014, **86**, 6188–6191, DOI: 10.1021/ac501290u.
  - 36 C. Yu, J. Zhang, J. Li, P. Liu, P. Wei and L. Chen, Fluorescent probe for copper(II) ion based on a rhodamine spirolactame derivative, and its application to fluorescent imaging in living cells, *Microchim. Acta*, 2011, **174**, 247–255, DOI: 10.1007/s00604-011-0623-2.
  - 37 S. J. Park, O. J. Shon, J. A. Rim, J. K. Lee, J. S. Kim, H. Nam and H. Kim, Calixazacrown ethers for copper(II) ion-selective electrode, *Talanta*, 2001, **55**, 297–304, DOI: 10.1016/S0039-9140(01)00420-9.
  - 38 L. K. L. Su, Chia-ching, Chuen-Her Ueng, Characteristics of Lariat Crown Ether-Copper(II) Ion-Selective Electrodes, *J. Chin. Chem. Soc.*, 2001, **48**, 733–738, DOI: 10.1002/jccs.200100105.
  - 39 S. Sadeghi, M. Eslahi, M. A. Naseri, H. Naeimi, H. Sharghi and A. Shameli, Copper Ion Selective Membrane Electrodes Based on Some Schiff Base Derivatives, *Electroanalysis*, 2003, **15**, 1327–1333, DOI: 10.1002/elan.200302807.
  - 40 Z. Szigeti, I. Bitter, K. Tóth, C. Latkoczy, D. J. Fliegel, D. Günther and E. Pretsch, A novel polymeric membrane electrode for the potentiometric analysis of Cu<sup>2+</sup> in drinking water, *Anal. Chim. Acta*, 2005, **532**, 129–136, DOI: 10.1016/j.aca.2004.10.061.
  - 41 S. Kamata, A. Bhale, Y. Fukunaga and H. Murata, Copper (II)-Selective Electrode Using Thiuram Disulfide Neutral Carriers, *Anal. Chem.*, 1988, **60**, 2464–2467, DOI: 10.1021/ac00173a006.
  - 42 E. Espada-Bellido, M. D. Galindo-Riaño, M. García-Vargas and R. Narayanaswamy, Selective chemosensor for copper ions based on fluorescence quenching of a schiff-base fluorophore, *Appl. Spectrosc.*, 2010, **64**, 727–732, DOI: 10.1366/000370210791666282.
  - 43 Y. Q. Weng, Y. L. Teng, F. Yue, Y. R. Zhong and B. H. Ye, A new selective fluorescent chemosensor for Cu(II) ion based on zinc porphyrin-dipyridylamino, *Inorg. Chem. Commun.*, 2007, **10**, 443–446, DOI: 10.1016/j.inoche.2006.12.023.
  - 44 Y. Rahimi, S. Shrestha and S. K. Deo, Metal affinity-based purification of a red fluorescent protein, *Chromatographia*, 2007, **65**, 429–433, DOI: 10.1365/s10337-007-0177-y.
  - 45 H. S. Kim and H. S. Choi, Spectrofluorimetric determination of copper(II) by its static quenching effect on the fluorescence of 4,5-dihydroxy-1,3-benzenedisulfonic acid, *Talanta*, 2001, **55**, 163–169, DOI: 10.1016/S0039-9140(01)00405-2.
  - 46 J. Coates, Interpretation of Infrared Spectra, A Practical Approach, *Encycl. Anal. Chem.*, 2004, 1–23, DOI: 10.1002/9780470027318.a5606.
  - 47 K. Mohanan, M. Thankamony and B. S. Kumari, Synthesis, spectroscopic characterization, and thermal decomposition kinetics of some lanthanide(III) nitrate complexes of 2-(N-o-hydroxyacetophenone)amino-3-carboxyethyl-4,5,6,7-tetrahydrobenzo[b]thiophene, *J. Rare Earths*, 2008, **26**, 463–468, DOI: 10.1016/S1002-0721(08)60119-2.
  - 48 M. Moore, J. T. Vandeberg and H. A. Flaschka, Tetraarylborates, *CRC Crit. Rev. Anal. Chem.*, 1971, **2**, 1–49, DOI: 10.1080/10408347108542760.
  - 49 J. D. Cuppett, S. E. Duncan and A. M. Dietrich, Evaluation of copper speciation and water quality factors that affect aqueous copper tasting response, *Chem. Senses*, 2006, **31**, 689–697, DOI: 10.1093/chemse/bjl010.
  - 50 D. C. Harris, *Quantitative Chemical Analysis*, W. H. Freeman, New York, 6th edn, 2003.
  - 51 S. Kamata, H. Murata, Y. Kubo and A. Bhale, Copper(II)-selective membrane electrodes based on o-xylylene bis (dithiocarbamates) as Neutral Carriers, *Analyst*, 1989, **114**, 1029–1031, DOI: 10.1039/AN9891401029.